

7.11 Experiment (M): Properties of cosmic muons

7.11.1 Tasks

1. Determination of the noise threshold of the detectors
2. Recording a pulse height spectrum
 - (a) Determination of suitable thresholds for muons and electrons/positrons
 - (b) Calibrating the pulse heights of the individual modules
3. Determination of the efficiency of the individual detector modules
4. Determination of the lifetime of the muon
5. Proof of the precession of the muon spin in the magnetic field and determination of the statistical significance



Figure 7.43: Setup of the cosmic muon experiment. The stack of three scintillation panels is seen on the right side. On the left side, the data acquisition electronics and the analysis computer can be seen.

7.11.2 Introduction

7.11.3 Composition of the cosmic rays

The primary cosmic rays, which originate partly in space and partly in the Sun, consist predominantly of protons (about 85%). It also contains a small fraction of α particles (about 12%), and with even lower abundance heavier nuclei (about 2% in total), electrons, and γ quanta.

It is a very high energy radiation. The energies of the particles range from 10^6 eV to 10^{21} eV. The primary spectrum has approximately the form

$$N(> E) = K \cdot \left(\frac{E}{E_0} \right)^{-\gamma} \quad \begin{aligned} E_0 &= 10^{16} \text{ eV} \\ K &= 3 \cdot 10^{-4} m^{-2} h^{-1} \\ \gamma &= 1.7 \dots 2.1 \end{aligned} \quad (7.128)$$

$N(> E)$ is the rate of particles with energies greater than E . The spectral index γ changes around $4 \cdot 10^{15}$ eV, at the so-called "knee".

When the primary cosmic radiation hits the Earth's atmosphere, secondary particles are generated by the interaction of the nucleons, which in turn initiate further reactions. Therefore, the composition of the cosmic radiation within the atmosphere is substantially different from the original one. It also changes with altitude. At sea level, there are almost no primary particles left.

The following processes take place: The primary nucleons first collide with air nuclei via the strong interaction and lose kinetic energy in the process. Large numbers of secondary, high-energy nucleons and pions are created, which themselves initiate further spallations through collisions. These processes stop only when the kinetic energy of the hadrons is no longer sufficient to produce pions. This happens at 300 MeV. A single primary nucleon thus produces a shower of very many strongly interacting particles, the so-called nuclear cascade. It does not reach the Earth's surface because the mean free path of pions and nucleons in matter is too small due to the strength of the interactions. Only a few protons and neutrons make it all the way.

The neutral pions of the nuclear cascade are unstable. They quickly decay electromagnetically into two γ quanta.

$$\pi^0 \rightarrow 2\gamma \quad \tau = 8.4 \cdot 10^{-17} \text{ s.} \quad (7.129)$$

The decay is very fast, so it takes place in the immediate vicinity of the nuclear cascade.

Those very energetic γ quanta are the starting point of the so-called **electromagnetic cascade**. At these high energies, the most probable process is pair production, whereas the Compton and photoelectric effects are negligible. In the Coulomb field of nuclei, particle-antiparticle pairs (see 3.2.2.3) are formed, most frequently the lightest of them, the electron-positron pair. Except for the small recoil energy of the nucleus, the leptons acquire the entire γ energy and are therefore themselves relativistic. Their direction of flight deviates only slightly from that of the incident quantum because of conservation of momentum.

Leptons lose their energy in matter either by ionization (chapter 3.1.1) or by bremsstrahlung (chapter 3.1.2). At high energies, bremsstrahlung predominates because it is proportional to $Z^2 \cdot E$, while ionization goes with $Z \cdot \ln(E)$. The two processes are equally likely at $800/Z$ MeV. Thus, the fast leptons generate Bremsquanta, which take over a large fraction of the energy and are preferentially emitted in the direction of flight. The Bremsquanta produce further lepton pairs, which in turn create γ quanta. In this way, the number of leptons doubles in each generation. A shower of leptons and γ -quanta is formed which propagates within a cone around the direction of flight of the primary particle. This electromagnetic cascade also terminates when the energy has become so small that the ionization processes (or Compton scattering) predominate. Only at primary energies $> 10^{12}$ eV appreciable parts of these electromagnetic air showers reach sea level.

The charged pions decay by the weak interaction into muons and muon neutrinos.

$$\begin{aligned}\pi^+ &\rightarrow \mu^+ + \nu_\mu & \tau = 2,60 \cdot 10^{-8} \text{ s} \\ \pi^- &\rightarrow \mu^- + \bar{\nu}_\mu\end{aligned}\tag{7.130}$$

Their average lifetime is much longer than that of the neutral pion. Therefore, the decay can take place at a considerable distance from the nuclear cascade. But also here, the mean free path length is not sufficient; again they hardly reach the Earth.

This is achieved by the muons created in pion decays. They are subject to the weak interaction and can induce nuclear transformations in matter. However, the effective cross sections for this are extremely small, so that their behavior is determined only by the electromagnetic interaction. Like electrons, they generate electromagnetic cascades, but with the essential restriction that due to their approximately 200 times larger mass, the probability of this is $4 \cdot 10^4$ times smaller (see chapter 3.1.2, Eq. 3.9). Their range is therefore greater than that of electrons. They reach the earth's surface and even penetrate deep into the earth.

The charged muons can also further decay via the weak interaction into an electron (or positron) with electron and a muon neutrinos:

$$\begin{aligned}\mu^+ &\rightarrow e^+ + \nu_e + \bar{\nu}_\mu & \tau = 2.19 \cdot 10^{-6} \text{ s.} \\ \mu^- &\rightarrow e^- + \bar{\nu}_e + \nu_\mu\end{aligned}\tag{7.131}$$

Their average lifetime is much longer than that of neutral pions.

Accordingly, the cosmic radiation on the earth's surface consists of two components. The penetrating one, which has a large mean free path, is called the hard component and consists of muons. The short-range, so-called soft component consists of electrons, positrons and bremsstrahlung quanta of the electromagnetic cascades. Only a small part comes from the decay of muons.

During the mean lifetime given in Eq. 7.131, an extremely relativistic muon travels approximately 600 m. This corresponds to the mean distance travelled by muons between their creation and their decay. It is too short to explain the abundance of muons at the earth's surface. This is solved by the theory of special relativity. Those lifetimes are valid in the rest system of the particles. However, in a system with a velocity v relative to the particle, time dilation becomes noticeable. The mean lifetime τ_E of the relativistic particle measured on earth is longer.

$$\tau_E = \frac{1}{\sqrt{1 - \frac{v^2}{c^2}}} \cdot \tau = \gamma \cdot \tau\tag{7.132}$$

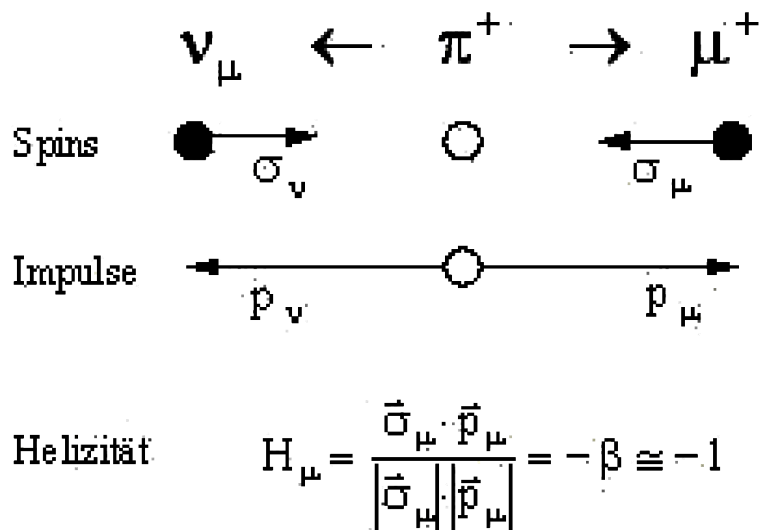
γ is the ratio of the total energy to the rest energy of the muon, c the speed of light. If E is the total energy, E_{kin} is kinetic energy and m_0 the rest mass, so is

$$\gamma = \frac{E}{m_0 c^2} = \frac{E_{\text{kin}} + m_0 c^2}{m_0 c^2} = \frac{1}{\sqrt{1 - \frac{v^2}{c^2}}}.\tag{7.133}$$

For extremely relativistic particles the rest energy is negligible compared to the kinetic energy, and one obtains

$$\gamma \approx \frac{E_{\text{kin}}}{m_0 c^2}\tag{7.134}$$

In numbers: for a muon of 10 GeV the mean lifetime on Earth is about 100 times longer than in the rest frame, so that this muon decays only after a mean distance of 60 km and thus has a good chance of reaching the ground.

Figure 7.44: Decay of the π^+ and helicity of the μ^+ .

7.11.4 The deceleration of muons in matter

The high-energy muons lose their energy in matter through Bremsstrahlung at the nuclei. Only at energies in the GeV range and below also ionization processes become noticeable through the Coulomb interaction. These processes are independent of the sign of the charge. However, at the end of their range, just before they come to rest, the positive and negative muons behave differently.

The negative muons, which differ from electrons only by their mass, are captured by the atoms mostly in excited states and land very quickly in the K-shell under emission of X-rays. The Pauli principle allows this, even if the shell is already occupied by electrons, because the particles are not identical. From there they are captured by the nucleus, where analogous to the K-capture of the electrons, the nucleons are transformed by the weak interaction. Thus, a second decay channel opens for the μ^- , which means that their average lifetime is lowered. In Cu, for example, one measures $\tau = 0.163 \mu\text{s}$. As a result of this strong reduction of the lifetime, in measurements of cosmic muons, where the positive and negative particles arrive with equal frequency, one records almost only μ^+ , since the μ^- are captured very quickly. In Cu, they are practically absent after a microsecond.

At low energies, the positive muons capture electrons from the atomic shells, with which they build a hydrogen-like structure in which the μ^+ replaces the hydrogen nucleus, it is called muonium. Subsequently, it can be ionized, rebuilt, alternating between capture and loss of an electron. The electrically neutral muonium is also further decelerated by collisions with electrons and atoms until it is finally thermalized.

The time scale on which these processes occur is short compared to the average lifetime of the muon. Deceleration due to scattering losses to a few keV takes about 10^{-10} s . The capture and ionization processes of the muonium last about $5 \cdot 10^{-13} \text{ s}$, after which it still has an energy of about 200 eV. At this energy, it becomes stable and thermalizes within another 10^{-12} s .

7.11.5 Muon polarization

The totality of muons in a given energy range is polarized in their momentum direction, i.e. the number of particles with a spin in parallel to their direction of flight is not equal to the number with an antiparallel spin. This is a consequence of the parity violation in the weak interaction and is explained in detail for the μ^+ as follows.

According to the V-A theory of the weak interaction there are only left-handed particles (negative helicity, i.e. spin antiparallel to the momentum direction) and right-handed antiparticles. The probability for the expectation values of these helicities is proportional to $\beta = v/c$. π^+ has spin 0 and ν_μ as a (nearly) massless particle must have a negative helicity. Because of the conservation of angular moment, the antiparticle μ^+ has no other choice but to be emitted with the wrong helicity, i.e. a negative one. This is the reason why the pion decays rarely ($\approx 10^{-4}$) into the lighter lepton, which would be preferred by the phase space. The probability for wrong helicity is lower for the highly relativistic electron.

The total energy of the muon in the pion's rest frame is

$$W_\mu = \frac{(m_\pi c^2)^2 + (m_\mu c^2)^2}{2m_\pi c^2} \quad (7.135)$$

The rest mass of the pion is 140 eV, that of the muon 106 MeV. This leads to a total energy of the muon of 110 MeV, leaving only 4 MeV as the kinetic energy.

On Earth, the muons have different energies depending on whether they are emitted in the direction of the pion's flight or in the opposite direction. For example, if the pions fly toward the detector with a total energy of 1 GeV, then the forward-moving muons have a total energy of 998 MeV, while those emitted backward have 662 MeV. The spin of the high-energy group is opposite to the direction of flight, while the spin of the low-energy particles is parallel to it. Since the decay of the pions is isotropic in their rest frame, there should be equal numbers of muons in each group. Now, if both groups are detected in the same way in a detector, the totality of muons is not polarized. If, on the other hand, one of the energies is discriminated and registered separately, one has complete polarization.

In reality, the pion spectrum is continuous, and the direction of incidence is also not perpendicular from above, but a distribution around this direction. The effect of the shape of the spectrum on the polarization can be easily understood. The muons whose lifetime is measured have been stopped in a Cu plate. They have lost only a few MeV of energy in the Cu, but much more before that on their way through the atmosphere. Since this path is of different length for the individual particles, depending on their place of origin, the muons ending in the Cu had energies in the GeV range with a broad but finite distribution when they were created. They have been emitted either forward or backward in the pion's rest frame. From relativistic kinematics we know that in the first case the kinetic energy of the pion must have been only a little bit, in the second case much larger than that of the muon. A numerical example: A muon with the (total) energy 1 GeV is created from a pion with 1.002 GeV for a forward decay, for a backward decay the pion must have 1.67 GeV.

The totality of stopped muons is polarized if the pion spectrum depends on the energy, because only then the number of muons produced at a fixed energy by forward and backward decays is not the same. It is known that the spectrum of pions in cosmic rays decreases with increasing energy, as expressed in Eq. 7.128. Therefore, for the μ^+ a negative polarization is to be expected, i.e. opposite to the direction of flight. In fact, for perpendicular incidence one measures the value $P = -1/3$ and this is only slightly dependent on the energy.

These considerations remain valid even if the condition of perpendicular incidence is no longer maintained. Then the polarization is averaged over the direction of incidence. In this case, the polarization is somewhat smaller, but always clearly different from zero.

There remains the question of the depolarization of the muons, which interact with matter after thermalization. The deceleration itself happens so fast that the muon, whether free or bound in the muonium, does not noticeably precess in external or internal magnetic fields and thus maintains the alignment. This is different after thermalization. Most of the time the muon remains (on average) in this state and is exposed to depolarizing interactions. The relaxation of the polarization depends strongly on the magnetic and crystal structure of the solids. In

paramagnetic metals, such as Cu, it is caused by the inhomogeneous magnetic fields of the nuclear moments or magnetic impurities. The relaxation time (this is the time in which the polarization has decreased on average to 1/e of its original value) in these materials is long. For Cu at room temperature, for instance, values greater than 50 μs have been measured. They are large compared to the average lifetime of muons. Therefore the depolarization is not noticeable.

7.11.6 A proof of muon decay

The end of the lifetime of a μ^+ is characterized by the appearance of a positron. The double differential spectrum of the positrons from the decaying μ^+ has the form

$$\frac{dN}{d\varepsilon d\Omega} = \frac{\varepsilon^2}{2\pi} \cdot [(3 - 2\varepsilon) - P \cdot (1 - 2\varepsilon) \cdot \cos \theta] \quad (7.136)$$

where $\varepsilon = E/E_{\max}$ is the positron energy in units of $E_{\max} = m_\mu c^2/2$, the maximum energy a positron can carry away in a decay, and θ is the angle between the spin of the muon and the momentum of the positron. P is the polarization of the muon.

This expression has the form

$$\frac{dN}{d\varepsilon d\Omega} = a \cdot (1 + b \cdot \cos \theta) \quad (7.137)$$

b depends on the positron energy and runs from $b = -1/3$ at $\varepsilon = 0$ through $b = 0$ at $\varepsilon = 1/2$ to the maximum value $b = 1$ at $\varepsilon = 1$. It states that the emission of the β^+ is not isotropic with respect to the spin of the μ^+ : the positron is preferentially emitted in the direction of the spin.

The spatial asymmetry is the greater, the more energetic the positrons are. Usually positrons with different energies are not detected with the same sensitivity. The low-energy ones do not reach the detector at all, because of their energy losses. For this reason, there is a lower threshold for the detection, on which, of course, the magnitude of the measured asymmetry depends. When integrating Eq. 7.137 over the energy one obtains

$$\frac{dN}{d\Omega} = k \cdot (1 + A \cdot \cos \theta) \quad (7.138)$$

k is a constant determined by the threshold. The size of the asymmetry depends on the chosen integration interval. When integrating over the whole spectrum, it is $A = P/3$. Using only the upper half results in $A = 0.44P$. For still higher thresholds A increases further until the upper limit $A = P$. Thus, it is advantageous to measure at high thresholds, where the effect is at its maximum. However, the counting rate becomes smaller and smaller, requiring a compromise.

The above expression has to be integrated over a finite solid angle if the angular distribution of the positrons is to be taken into account. Because of the averaging over the angle θ , the asymmetry decreases, e.g. to half when integrating over the half-space.

7.11.6.1 The precession of muons in the magnetic field

A magnetic moment associated with the angular momentum \vec{J} .

$$\vec{\mu} = \gamma \cdot \vec{J} \quad (7.139)$$

in a magnetic field \vec{B} has the equation of motion

$$\frac{d\vec{J}}{dt} = \vec{\mu} \times \vec{B} \quad (7.140)$$

from which it follows that the magnetic moment precedes around the field direction with the angular frequency

$$\omega = \gamma \cdot B \quad (7.141)$$

The precession is counterclockwise when looking in the direction of the magnetic field. The gyromagnetic ratio γ of a particle is

$$\gamma = \frac{g \cdot \mu_B}{\hbar} \quad (7.142)$$

Where μ_B is the Bohr magneton. For an electron this is

$$\mu_B(\text{Electron}) = \frac{e \cdot \hbar}{2 \cdot m_e} = 9,273 \cdot 10^{-24} \frac{\text{J}}{\text{T}} \quad (7.143)$$

for a muon

$$\mu_B(\text{Muon}) = \frac{e \cdot \hbar}{2 \cdot m_\mu} = \frac{m_e}{m_\mu} \cdot \mu_B(\text{Elektron}) = 4,485 \cdot 10^{-26} \frac{\text{J}}{\text{T}} \quad (7.144)$$

The dimensionless quantity g is called the Landé factor. It is different for the orbital angular momentum of a charged particle and its spin. In the first case it is exactly equal to one, in the second case it is 2 plus higher order corrections. It can be determined by measuring the precession frequency of a free particle in a magnetic field

$$g = \frac{\gamma \cdot \hbar}{\mu_B} = \frac{\hbar \cdot \omega}{\mu_B \cdot B} \quad (7.145)$$

7.11.7 Principle of measurement

The measurement of the precession frequency of μ^+ is similar to the measurement of the mean lifetime, only extended accordingly. The deceleration of the muon in the detector marks the start time of the measurement, and the stop time is defined by the appearance of the positron from the decay. If the measurement is repeated for many muons, the number $N(t)$ of particles decaying at time t is obtained. It obeys the exponential law for radioactive decay

$$N(t) = N_0 \cdot e^{-t/\tau} \quad (7.146)$$

τ is the mean lifetime and N_0 is the number of muons stopped in the detector during the measurement time. As long as we just want to determine τ , it is sufficient to simply detect the positrons regardless of their energy and direction. For this purpose the detector can be used as stop target.

To measure the precession, it is necessary to extend the measurement with two aspects. First, a constant magnetic field is placed over the stop target transverse to the direction of muon incidence, in which the spins precess. Second, only positrons emitted in a particular direction are measured. The count rate is then modulated with the precession frequency; it is largest when the muon spin points in that direction, smallest when pointing in the opposite direction. The angle θ in Eq. 7.138 is then no longer constant in time, it has to be replaced by the precession angle ωt .

The number of positrons detected at a time t is obtained by combining Eq. 7.138 and Eq. 7.146.

$$N(t) = K \cdot e^{-t/\tau} \cdot [1 + \bar{A} \cdot \cos(\omega t + \delta)] \quad (7.147)$$

The exponential function describes the decrease due to the decay. The expression in the parenthesis describes the modulation due to the precession. The bar in the asymmetry \bar{A} indicates that this quantity is obtained by averaging over the geometry of the detector. It is time dependent because of the depolarization of the stopped μ^+ and is sometimes written as

$$\bar{A} = \bar{A}_0 \cdot e^{-t/T_R} \quad (7.148)$$

with T_R the relaxation time of the polarization. For Cu, the asymmetry can be assumed to be constant within the measurement time.

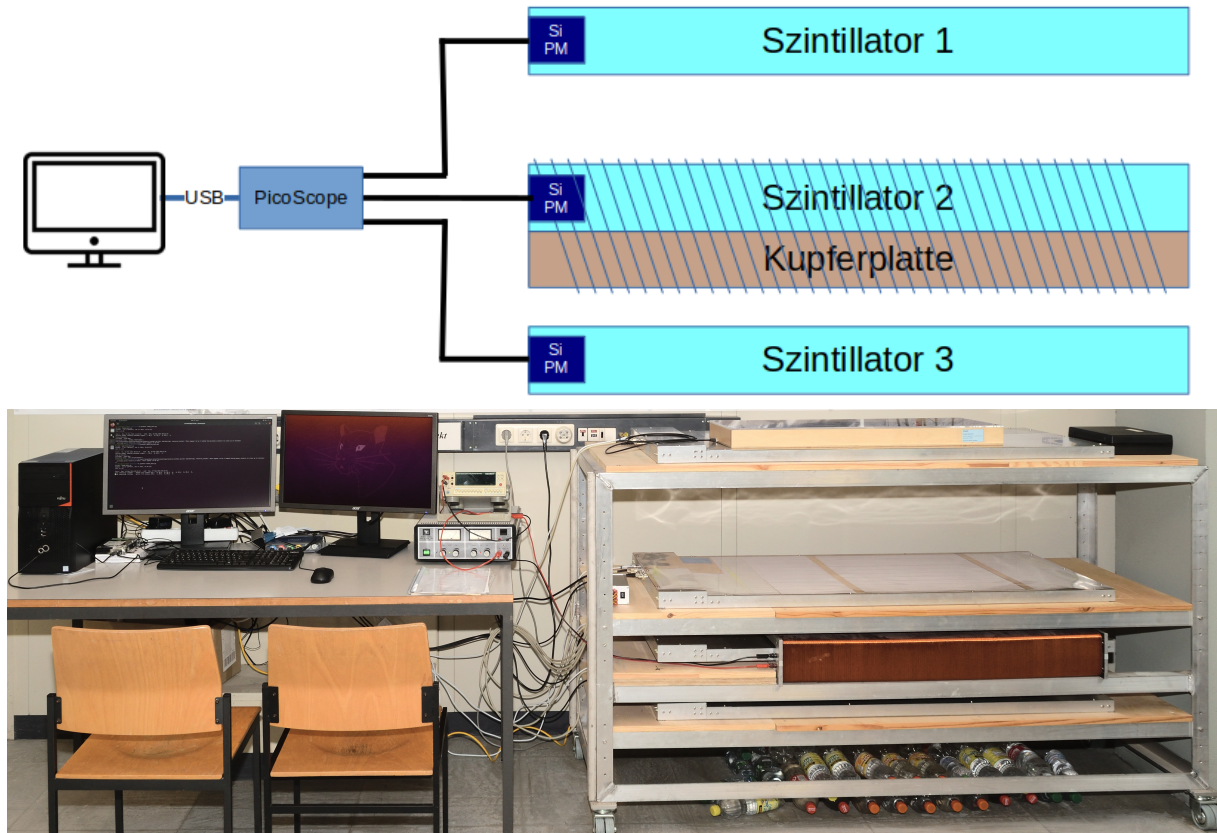


Figure 7.45: Top: sketch of the setup. Bottom: experimental setup in the lab.

7.11.8 Setup and execution

The experiment was revised in 2021 and the new setup is sketched in Fig. 7.45. It consists of three modules lying one above the other, each with 10 horizontally adjacent scintillator blocks made of plastic, each 1 cm thick, 5 cm wide and 93.5 cm long, which are connected via internal light guides (wavelength shifter) to a Si-photomultiplier (see Fig. 7.46). Between the second and the third scintillator module there is a 2.5 cm thick copper plate, in which the μ^+ should preferably be stopped due to the higher density. The second module and the copper plate are located within a 1 m long coil with 960 windings. The signals from the three Si-photomultipliers are digitized with a 4-channel USB oscilloscope (PicoScope 3404D) and transferred to a PC (Linux). As described in chapter 5.5, in this experiment the analog signal is digitized directly using a USB oscilloscope and the analysis of pulse height and coincidence then takes place in the software and is therefore highly configurable. The transfer of data from the USB oscilloscope to the PC requires a certain amount of time during which no new data can be digitized (cf. dead time of analog circuits). It is therefore not advisable to permanently transfer all data to the PC. Otherwise you would lose potentially relevant data that fall into the dead time. This loss can be minimized by setting a trigger threshold above which the signal must be, in order to be considered relevant. Only a certain time range before and after the signal was above this

threshold (trigger time) is then transferred to the PC where it is further evaluated. A good way of finding a suitable threshold is provided by the manufacturer's PicoScope software, which allows you to clearly test and graphically evaluate different thresholds. An optimal operating point for this threshold is just above the inherent noise of the detector modules and below all signal peaks assumed to be relevant. The processing, filtering and saving of the data in the following parts of the experiment is done with the help of a modular software specially written in the language *Python*, the structure of which is explained in more detail below. All relevant parameters, such as the signal thresholds and coincidence conditions, can be set for the individual measurements using configuration files in *yaml* format (text files with a predefined syntax that can be edited with a standard text editor).



Figure 7.46: Scintillator module with ten scintillating bars, Si-PM, and electronics.

For the following measurements it is necessary to determine thresholds for typical muon and positron signals. Therefore, a pulse height spectrum is first recorded for all detected signals from all modules. A signal is saved as soon as it is above the trigger threshold of the USB oscilloscope in the top detector module. Furthermore, signals from other detector modules are registered and stored if they occur in coincidence with the top module. If a signal occurs in each of the detectors at the same time, it can be assumed with high probability that it was triggered by a muon. These "throughgoing muons" are suitable for calibrating the signal height of the individual detector modules, since their pulse height distribution must be the same in all modules. In order to obtain a robust estimated value for the individual modules, the top and bottom 10

Furthermore, the efficiency of the individual detector modules can be estimated from the collected measured values. Due to strict constraints on the coincidence of two signals from two different modules, it is very unlikely that they were accidentally triggered by two independent particle events. Since the detector modules are precisely aligned on top of each other, it can generally be assumed that a signal in the top and bottom detectors is a significant indication of a throughgoing muon, and consequently a signal should also be seen in the middle detector. The efficiency of the middle detector can be calculated from the ratio of events with a signal in all three detectors to events in which only the top and bottom detectors responded. This method called "tag and probe" can also be used with unequal detector modules, as long as it is ensured that an event with a coincidence signal in the top and bottom detector must always trigger a signal in the detector to be tested.

The signature of a muon stopped in the Cu plate is $1+2+\bar{3}$, i.e. a coincidence of the two upper ones in anticoincidence with the lower scintillator. Such an event triggers the start of the lifetime measurement. The end of life is marked by the appearance of a positron in either scintillator 2 or 3. The random coincidences with passing muons are suppressed when an anticoincidence with the counter opposite is required. The signals $2 + \bar{3}$ and $3 + \bar{2}$ are equivalent, the best signature

for the stop is $1 + 2 + \bar{3}$. It improves the ratio of true to random coincidences, albeit with a loss of counting rate, because it shifts the threshold for e^+ detection to higher energies in the region of greater asymmetry.

In order to keep the measurement time for the lifetime measurement as short as possible, the decay function is fitted to the measurement data using the maximum likelihood method instead of being fitted to a histogram.

You are required to work on this evaluation with the help of your supervisor while the measurement is running. For this purpose, a prepared Jupyter notebook is provided that uses the packages *kafe2* and *PhyPraKit*. An excellent source of information are the examples of the two Python packages on the Internet, as well as the lectures on computer application for bachelor students.

In order to measure the precession frequency, the magnetic field is turned on and data is recorded for at least a week. The signature is the same as in the lifetime measurement, but a strict distinction must now be made between positrons emitted upwards and downwards, since the modulation of the two decay functions is phase-shifted by 180° (i.e. they would just cancel out). Since the modulation signal due to the precession of the muon spin is extremely weak and the fitting of the decay function proves to be difficult due to the large number of free parameters, the Landé factor cannot be reliably determined with the data from one week. Therefore, the task is a simple hypothesis test of whether an expected precession modulation is present and how significantly it differs from a decay function without modulation. Again, it is recommended to use packages such as *kafe2* or *PhyPraKit* for the fitting to function, since most of the other simple tools do not provide the required functionality for analyzing likelihoods. Follow the analysis strategy outlined below, which is also provided as a template in a Jupyter notebook:

1. Discard events with decay times smaller than $0.6 \mu\text{s}$ because they are dominated by nuclear captures of negative muons with shorter decay times.
2. Calculate the expected oscillation frequency ω from the magnetic field of the coil and the literature values and plot the decay function with expected values and a modulation amplitude of $\bar{A} \approx 15\%$.
3. Plot the decay times in a histogram using as few bins as possible, but still enough to safely resolve the modulation (see plotted decay function).
4. Fit a decay function *without* modulation to the histogram and determine the decay time of the muon τ and the background portion f_{bkg} .
5. Now fit the decay function *with* the modulation to the histogram, fixing all free parameters except the modulation amplitude \bar{A} to the literature values or the parameters found in the previous fitting.
6. Use the additional variables to include only those decay times in the histogram that show a pronounced modulation signal (e.g. only events with a stop signature $1 + 2 + \bar{3}$, or only events with a certain minimum/maximum signal height for muon and/or positron).
7. If you have found good cuts in the previous step with \bar{A} as large as possible and $\sigma_{\bar{A}}$ as small as possible, calculate the log-likelihood ratio nL between the decay function with modulation and the decay function without modulation. As a simple statistical test, $2 \cdot nL$ follows a χ^2 distribution with as many degrees of freedom as the two models differ in the number of fitted parameters (in this case one parameter). For the special case with one parameter, $z = \sqrt{2 \cdot nL}$ can also be considered; the z value indicates by "how many standard deviations" σ of the discriminating parameter the two models differ.

The software for data acquisition uses a general basic package (`mimoCoRB` = "multiple-in, multiple-out Configurable RingBuffer"), which can also be used in other problems, to which experiment-specific code must be added.

The `mimoCoRB` package provides a central component of any data acquisition system, which is used to record and process data from random processes before it is written to a permanent storage. Typical examples are digitized waveform data as they arise from detectors in nuclear, particle and astroparticle physics or in quantum mechanical measurements of single particles, for instance from photo-multiplier tubes, Geiger counters, avalanche photodiodes or modern SiPMs.

The random nature of such processes and the need to minimize read-out dead-times requires the use of an input buffer into which data is copied rapidly. While a data source feeds the data into the buffer, the subsequent processes are supplied with an almost constant stream of data in order to filter, reduce, analyze or visualize them. Such so-called consumer processes can be mandatory, i.e. they have to process all data. In this case, data acquisition pauses when the input buffer is full and a mandatory consumer is still busy processing. A second type of consumer, an "observer" process, receives a copy of the data only upon request without interrupting the data collection. A typical example of this is the graphical display of a subset of the recorded data.

Although it is possible to use the buffer manager in the `mimoCoRB` package directly, it makes more sense and is easier to use specially defined access classes with a well-defined user interface. The class structure is shown in Fig. 7.47. The main configuration shown at top left is in the working directory; the experiment-specific code indicated in the boxes with blue background and the necessary configuration files as well as the output data reside in subdirectories.

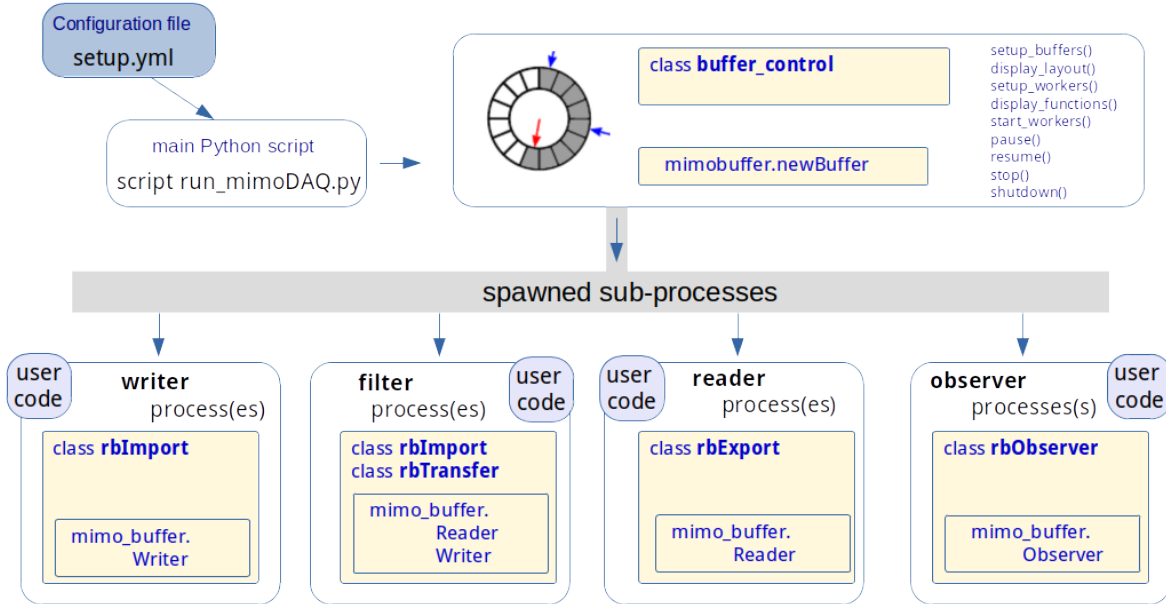


Figure 7.47: Structure of the software package `mimoCoRB`

The structure of the buffers and functions for measuring the muon lifetime is shown in Fig. 7.48.

The first buffer contains all data from events that met the oscilloscope's trigger condition. The filter reads this raw data, searches for double pulses of stopped and subsequently decayed muons and writes this raw data into the second buffer. The parameters of the pulses found are stored in the third buffer. Two further reader processes then write this data from the ring buffer to the permanent storage device (file on disk). Additional configuration options can be used to

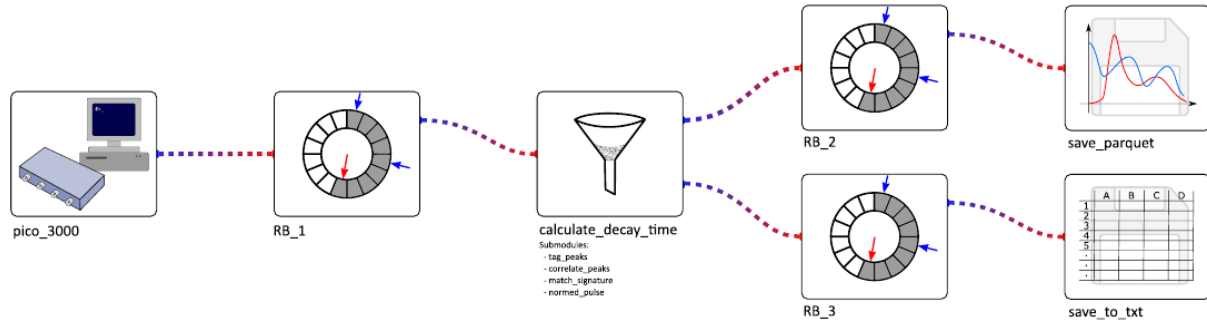


Figure 7.48: Software setup for the measurement of the muon lifetime.

launch processes that plot the raw data from the first or second buffer, or create histograms of variables in the third buffer and display updated versions of them in real-time.

The code with the configuration shown is started by typing

`./run_daq.py lifetime_setup.yaml`

on the command line. In the configuration script more configuration files are specified, which you can find in the subdirectories of your working directory. There, you can also find the experiment-specific code and Jupyter notebooks for the data evaluation:

```

|--> <working directory> # Location of main configuration files
|
| --> analysis/ # Jupyter notebooks for evaluation
| --> config/   # Configuration files in yaml format
| --> modules/  # experiment-specific Python code
| --> target/   # output files
  
```

The complete package `mimoCoRB` including an executable example based on simulated data, as well as the documentation can be found on the `gitlab` server of KIT under the URL <https://git.scc.kit.edu/etp-teaching/mimoCoRB>.

To support the evaluation, there are Jupyter notebooks for evaluating the pulse height spectra (`spectrum.ipynb`), for measuring the lifetime (`lifetime.ipynb`) and one spin measurement template (`spin_for_students.ipynb`) in subdirectory `analysis/`. The first two notebooks are almost completely operational and should be used on the day of the experiment to set the thresholds and coincidence conditions and to measure the lifetime. The included code sections also serve as examples and templates for the evaluation of the long-term measurement to provide prove of the muon spin and can be transferred to the notebook provided for this purpose.

Remark: This experiment has been rebuilt with new data acquisition and analysis methods. Therefore, details may still be adjusted over time, with which the supervisor will familiarize you.

7.11.9 Literature

Introductory chapters 1 - 6 in this script
 Muons, cosmic rays [30], [31], [32], [43], [44]
 Detectors [18], [19]